IET Nanobiotechnology

Research Article

IET Journals
The Institution of Engineering and Technology

Co-condensation synthesis of well-defined mesoporous silica nanoparticles: effect of surface chemical modification on plasmid DNA condensation and transfection

ISSN 1751-8741
Received on 28th March 2017
Revised 20th July 2017
Accepted on 2nd August 2017
E-First on 18th September 2017
doi: 10.1049/iet-nbt.2017.0078
www.ietdl.org

Mahdokht Mahmoodi[1,2], Abbas Behzad-Behbahani[1] ✉, Sadigheh Sharifzadeh[1], Samira Sadat Abolmaali[3,4], AliMohammad Tamaddon[3,4]

[1]Diagnostic Laboratory Sciences and Technology Research Center, School of Paramedical Sciences, Shiraz University of Medical Sciences, Shiraz, Iran

[2]Department of Medical Biotechnology, School of Paramedical Sciences, Shiraz University of Medical Sciences, Shiraz, Iran

[3]Center for Nanotechnology in Drug Delivery, School of Pharmacy, Shiraz University of Medical Sciences, Shiraz, Iran

[4]Department of Pharmaceutical Nanotechnology, School of Pharmacy, Shiraz University of Medical Sciences, Shiraz, Iran

✉ *E-mail: behzadba@sums.ac.ir*

Abstract: Chemically modified mesoporous silica nanoparticles (MSNs) are of interest due to their chemical and thermal stability with adjustable morphology and porosity; therefore, it was aimed to develop and compare the MCM-41 MSNs functionalised with imidazole groups (MCM-41-Im) to unmodified (MCM-41-OH) and primary amine functionalised (MCM-41-NH_2) MSNs for experimental gene delivery. The results show efficient transfection of the complexes of the plasmid and either MCM-41-NH_2 or MCM-41-Im. Furthermore, following transfection of HeLa cells using MCM-41-Im, an enhanced GFP expression was achieved consistent with the noticeable DNase1 protection and endosomal escape properties of MCM-41-Im using carboxyfluorescein tracer.

1 Introduction

Gene therapy is a method for improvement of genetic disorders and some other diseases such as cancers by correcting the genes which cause dysfunction [1, 2]. Although such diseases could be treated or their progression halted theoretically through the use of gene therapy, some limitations exist due to the imperfect methods suggested for an effective gene delivery [3, 4]. Thus, development of an optimised process for transferring the gene to intracellular target is a crucial step for the progression of gene therapy [5].

As some serious defects such as insertion mutation and the immunogenic reaction may exist using viral gene delivery method, non-viral methods have attracted more attention [4]. Among several non-viral methods, development of new delivery solutions based on nanotechnology is promising [6, 7].

Recent advancement in nanotechnology has revolutionised the subject of transferring biomaterials to target cells and tissues by manipulating biocompatible complexes with genetic materials [8, 9], with immense loading efficiency, consistency, and the ability to accomplish multiple applications synchronically [10, 11]. There are some beneficial properties for new engineered carriers via nanotechnology such as conservation and control release of payloads, low cytotoxicity, and safer internalisation to target cells [12]. During gene transfection, nanomaterials acting as gene carrier can internalise genetic materials to cells more sufficiently than other conventional methods with less toxicity [13–15]. They can also present their burden to the nucleus of target cells while remaining intact [16, 17].

In recent years, uniformity and adjustability of the pore size of highly dispersed porous materials have attracted much attention [12, 18, 19]. Ordered mesoporous silica with a pore size of 2–50 nm is a particular class of these nanocarriers that are generally synthesised in the presence of surfactant-type organic template around a silica framework [20]. Some desirable features of mesoporous silica nanoparticles (MSNs), such as chemical inertness, the simplicity of production, hardiness, the special design of porous and adjustable surface chemistry, allow them to be considered as ideal vehicles to transfer biomolecules [21]. This special architecture raises the efficiency of the surface of MSN to carry different types of cargoes in their inner pores or external surfaces [22].

The surface of MSN can be modified by functional groups in order to condense nucleic acids and to facilitate cellular uptake and endosomal escape with low toxicity [23–25]. Recent developments have been made for gene therapy application through the use of MSNs [21]. Surface functionalised (modified) MSNs thorough phosphonate [26] poly L-arginine [27], poly-ethyleneimine [28–30], cyclodextrin [31], poly-2-(dimethylamino) ethyl-methacrylate [32], and poly-L-lysine [33] have been reported previously to improve the transfection of siRNA, DNA, or controlled release of drugs to the cells for the purpose of cancer therapy. Barkalina *et al.* presented a formulation of poly ethyleneimine coated and –NH_2 functionalised MSNs, which had been loaded with boar sperm. The carrier has been shown to be successful in the delivery of biomaterials into mammalian sperms without any negative effect on the major parameters of sperm function [23]. Recently, chemical modification by L-histidine using 'grafting to' approach shows a significant enhancement of MSNs for gene transfer in an Achilles tendon in vivo [34].

Introducing amine groups via 'co-condensation' method on the surface of MCM-41 can also improve some carrier characteristics such as DNA condensation and cellular uptake but may exert cytotoxicity [34, 35]. Recently, Farjadian *et al.* [36, 37] reported novel synthetic route in preparation of MSNs which resulted in formation of controlled-sized nanoparticles with nanosphere sizes <50 nm. In this study, a surface chemical entity of a special type of MSNs (well-defined MCM-41) was altered via 'co-condensation' approach using silane coupling agents for acquiring a more efficacious and safer gene delivery system [36]. Therefore, we aimed to develop MCM-41 MSNs functionalised with imidazole (MCM-41-Im) in comparison to primary amine (MCM-41-NH_2) and unmodified MSNs (MCM-41-OH) for experimental delivery of a reporter gene plasmid (E-GFP) in HeLa cells.

2 Materials and methods

2.1 Materials and instrumentation

Tetraethyl orthosilicate (TEOS), (3-aminopropyl) triethoxysilane (APTES), and triethoxy-3-(2-imidazolin-1-yl)propylsilane were obtained from Sigma-Aldrich. Cetyl trimethylammonium bromide (CTAB) was purchased from Daejung Chemical (Korea), Metafectene from Biontex (Germany), cell culture medium (DMEM, Dulbecco's modified Eagles medium), foetal bovine serum (FBS), kanamycin, penicillin–streptomycin antibiotic, and dimethyl sulphoxide (DMSO) from GIBCO/BRL Life Technologies. Freshly prepared deionised water (Milli-Q3, Millipore, UK) was used in all experiments. All other reagents were of analytical grade.

Synthesised MSNs Fourier transform infrared spectroscopy (FTIR) spectra were gathered using FTIR spectrometer (Burker, vertex70, Germany) over the spectral region of 400–4000 cm^{-1}. Collection of the samples X-ray diffraction (XRD) patterns was completed using an X-ray diffractometer (D8 Advance, Bruker) at 30 mA and 30 kV. The data from diffraction angles (2θ) below 10° was gathered. CHN Elemental Analyzer (Termo finningan, Germany) was used for determination of carbon (C), hydrogen (H), and nitrogen (N) content of the modified MSNs. Millimole N per gram of each sample was used for *N/P* calculations [38]. The samples' pores characteristics were examined through the determination of nitrogen adsorption at −196°C. Before analysis, MSNs was completely degassed for 12 h at 350°C. The determination of pore characteristics was done in accordance with Brunauer–Emmett–Teller (BET) via plotting the adsorption isotherms. Characterisation of the synthesised MSNs was done using a FESEM (MRA3, TESCAN, USA) and HRTEM (PHILIPS EM 208, USA) in order to determine the particle size and morphology. Prior to imaging, samples were sputter-coated with gold. Dynamic light scattering (DLS) (Nanoflex, Microtrac, Germany) and streaming potential (Zeta-check, Microtrac, Germany) were employed to measure hydrodynamic diameter and zeta potential of the samples having been dispersed by ultrasonication (UP100H, Hielscher, Germany), respectively, carbon and nitrogen contents of the samples were determined by Elemental analyzer (FlashEA 1112, Thermo Finningan, Germany).

2.2 MSN (MCM-41) synthesis

Preparation of MCM-41 was carried out using a two-step preparation method [36, 37]. First, 0.31 mmol CTAB was dissolved at 60°C in 0.5 M NH_4OH solution while stirring vigorously for 30 min. Then, a dilute solution of TEOS in ethanol (0.2 M) was added drop-wise during 20 min. After 4 h continuous stirring, a concentrated ethanolic solution of TEOS (1 M) was added. Solution ageing took place over 24 h at 60°C. Collection (via sintered glass filter), washing, and re-dispersion of the samples with deionised water and ethanol were undertaken several times following drying in an oven at 80°C overnight. Acidic ethanol extraction (1 g HCl/50 ml ethanol for 48 h) was used to remove the surfactant templates, which was followed by a washing and drying cycle.

2.3 Chemically modified MCM-41 synthesis

MCM-41-NH_2 and MCM-41-Im particles were prepared according to the aforementioned procedure using 'co-condensation' synthesis method [36, 37]. In order to functionalise MCM-41 with primary amine groups, 0.5 M NH_4OH was used to dissolve CTAB (0.32 mmol) for 20 min at 65°C. Then, ethanolic solution of TEOS (0.32 mmol) and APTES (0.11 mmol) at 0.2 M total concentration was added simultaneously under stirring. A concentrated ethanolic TEOS and APTES solution (3:1 TEOS/APTES molar ratio, 1 M total concentration) were then added drop-wise after a 4 h stirring period. Solution ageing took place over 24 h at 60°C. Extraction of surfactant templates was accomplished in acidic ethanol similar to the procedure used for the preparation of unmodified MCM-41 nanoparticles. MCM-41-Im was also synthesised with triethoxy-3-(2-imidazolin-1-yl) propylsilane added instead of APTES in 1:3 molar ratio with respect to TEOS. To complete the reaction, a similar procedure was followed.

2.4 Plasmid cloning and extraction

pEGFP-C1 expression vector (4700 bp) containing CMV promoter, kanamycin resistant gene, and EGFP sequence was cloned in *Escherichia coli* BL-21 bacteria. After transformation of plasmid DNA into *E. coli*, bacteria were grown on LB agar containing kanamycin. Bacteria containing plasmids were selected and individual colonies were immersed in a sterile culture tube containing LB broth supplemented with antibiotic. Tubes were incubated in an orbital shaker incubator at 37°C for at least 2 h. When the solution reached a reasonable level of turbidity, plasmid extraction was performed using Maxi-prep plasmid extraction kit (Thermo-Fisher Scientific). The yield concentration was measured by PicoDrop spectrophotometer (Pico 200, Transferpette, Germany). The consistency of extracted plasmid was investigated on agarose gel (1%) using 1 × TBE buffer (50 mM Tris, 100 mM borate, 10 mM EDTA, pH 8.2).

2.5 pDNA/MSN formulation

pDNA/MSN complexes were prepared at various *N/P* mole ratios (0.1–5) of the modified MCM-41 nitrogen to the plasmid phosphate. Accordingly, the concentrated solution of MCM-41 MSNs in 1 M HEPES (20 mg/ml) sonicated for 30 min. Depending on *N/P* proportions, different volumes of the MSN stock solution were added to 1 µg plasmid solution and incubated at 4°C for 2 h. The complexes of pDNA/MSN were freshly prepared before each experiment.

2.6 Agarose gel retardation assay

The complex formation between pDNA and MSNs (either MCM-41-NH_2 or MCM-41-Im) was investigated by ethidium bromide agarose gel retardation assay [34, 38]. To determine the optimum *N/P* molar ratio defined by the maximum level of plasmid DNA retardation in the agarose gel with the minimum quantity of MSNs, the preparations at various *N/P* ratios were mixed individually with a loading dye before running the gel at 100 V for 45 min.

2.7 DNase1 protection assay

Evaluation of plasmid DNA protection from DNase 1 digestion (MBI Fermentas, Germany) was performed before and after forming a complex with modified MSNs in various *N/P* equivalents, where free plasmid DNA was served as a control [17]. All preparations were treated with 2 µl DNase1 in 20 µl final volume and incubated at 37°C for 30 min, followed by 10 min incubation at 65°C for enzyme deactivation. Products were run in agarose gel at 100 V for 45 min. The DNA resided in the wells was extracted by Plasmid DNA extraction kit (Vivantis, Malaysia). The extracted plasmid DNA was loaded again in agarose gel and compared with intact plasmid DNA bands in the gel following electrophoresis.

2.8 Cell culture

HeLa cells (human cervical cancer cell lining) were purchased from Cell Bank of Pasteur Institute (Iran), and cultured in DMEM with 10% (v/v) FBS and 1% (v/v) penicillin–streptomycin. The cells were maintained at 37°C/5% CO_2 and subcultured every other day.

2.9 Cytotoxicity

Cell cytotoxicity of unmodified and modified MCM-41 (MCM-41-NH_2 and MCM-41-Im) was examined with a tetrazolium (MTT)-based colorimetric assay. Briefly, HeLa cells were seeded in 96-well plates at the density of 10^4 cells per well and incubated for 24 h at 37°C/5% CO_2; MSNs of various concentrations in the range of 1–30 mg/ml were prepared by serial dilutions using growth culture

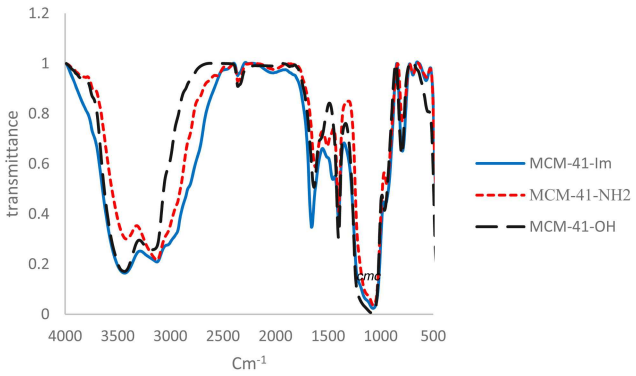

Fig. 1 *FTIR spectra of unmodified MCM-41 (MCM-41-OH) and the corresponding particles modified with primary amine (MCM-41-NH_2) and imidazole (MCM-41-Im)*

Table 1 CHN analysis of the modified types of MCM-41

Component name	Average in MCM-41-NH_2, %	Average in MCM-41-IM, %
nitrogen	4.16	5.9
carbon	11.8	15.6
hydrogen	3.2	3.8

Table 2 Surface characteristics of MSNs before and after modification

Type of MSN	SBET, m^2/g	Vt, cm^3/g	WBJH, nm
MCM-41-OH	1025	1.5	2.9
MCM-41-NH_2	975	0.9	2.6
MCM-41-Im	780	0.7	1.6

medium. The cells treated with MSN-free medium were considered as negative control. The medium was replaced by the MSN containing media and incubated for a further 24 h, followed by addition of 20 µl MTT solution (5 mg/ml) into each well. The growth medium was removed after 4 h incubation and then 150 µl DMSO was added to each well and kept at 37°C environment for 30 min. The light absorbance was measured at 570 nm using a microplate spectrophotometer (Power Wave XS, Biotek, USA). The averaged absorbance readings were divided by the corresponding absorbance of control cells (no treatment) to calculate cytotoxicity. The cytotoxicity of the MSNs/pDNA complexes prepared was examined similarly after 24 h incubation of the cells with various *N*/*P* ratios of MSN to pDNA. The corresponding treatments of Metafectene®/E-GFP plasmid complexes prepared according to the manufacturer's instruction [39] and E-GFP plasmid alone (MSNfree) were considered as positive and negative controls, respectively. Each experiment was run in triplicate.

2.10 E-GFP expression

Quantitative determinations of E-GFP expression were carried out using a FACSCalibur flow cytometer (Becton Dickinson, USA). All cell samples were suspended in PBS in order to disperse cell-clumps just prior to analysis. Voltage and gain settings were obtained for FL1 (green fluorescence) readings (582 and 1.00 in log mode) and for FSC (forward scatter) readings (E00 and 1.00 in linear mode) were recorded. Typically, 10^4 cells were analysed per sample. CELL Quest software (Becton Dickinson, USA) was used to perform data acquisition and subsequent analysis.

2.11 Endosomal escape

Carboxy fluorescein was used as a membrane impermeable fluorophore to monitor the endosomal membrane rupture following the uptake of MSNs [40]. A number of 10^4 cells were seeded in 6-well plates.

Following 24 h incubation at 37°C/5% CO_2, the cells were treated with 0.5 mg/ml carboxy fluorescein either alone (control cells) or with unlabelled MCM-41-NH_2 and MCM-41-Im (0.5 and 1 mg/ml) in complete culture medium without phenol red. After a 4 h incubation at 37°C, the cells were washed three times, trypsinised, re-suspended in 500 µl of sodium monensin in ice-cold PBS (20 µM), and analysed by FACS Calibur flow cytometer.

3 Results

3.1 Synthesis and characterisation of MSNs

To verify the presence of amine and imidazole functional groups in the synthesised MSNs, FTIR spectroscopy was carried out. The asymmetric stretching vibrations of (Si–O–Si) can be observed at ~1080–1100 cm^{-1} for all MSNs. Intense peaks between 3200 and 3500 cm^{-1} and ~1650 cm^{-1} are related to OH stretching and scissor bending vibration of H-bonded water molecules [41]. The modified structure with APTES reagent resulted in the appearance of the bands at 3100 and at 1484 cm^{-1} which are attributed to C–H and N–H stretching vibration of aminopropyl anchored on the surface of silica nanoparticles. The FTIR of MCM-41-Im showed the characteristic bands at 1650 1458 and 1505 cm^{-1} belonging to N–C = NC–N and C = C of the imidazole ring, respectively (Fig. 1) [42].

CHN analysis was performed to estimate the degree of chemical modification, confirming the presence of amine and imidazole nitrogen atoms (Table 1). Accordingly, nitrogen content was estimated 2.9 (mmol/g) for MCM-41-NH_2 and 4.2 mmol/g imidazole groups for MCM-41-Im.

The nitrogen absorption–desorption technique and BET calculations were also performed to obtain volume (Vt cm^3/g) of the synthesised structures as well as the surface area (i.e. SBET m^2/g) data as given in Table 2. The MSN samples possess a high level of SBET, Vt, and WBJH. Furthermore, the results show a modest reduction in SBET, Vt, and WBJH after functionalisation.

The morphological characteristics of synthesised MSNs were determined by FE-SEM and HRTEM (Figs. 2 and 3). The micrographs showed that MSN had spherical shapes with mean diameters of ~42 nm for MCM-41, 47 nm for MCM-41-NH_2, and 37 nm for MCM-41-Im.

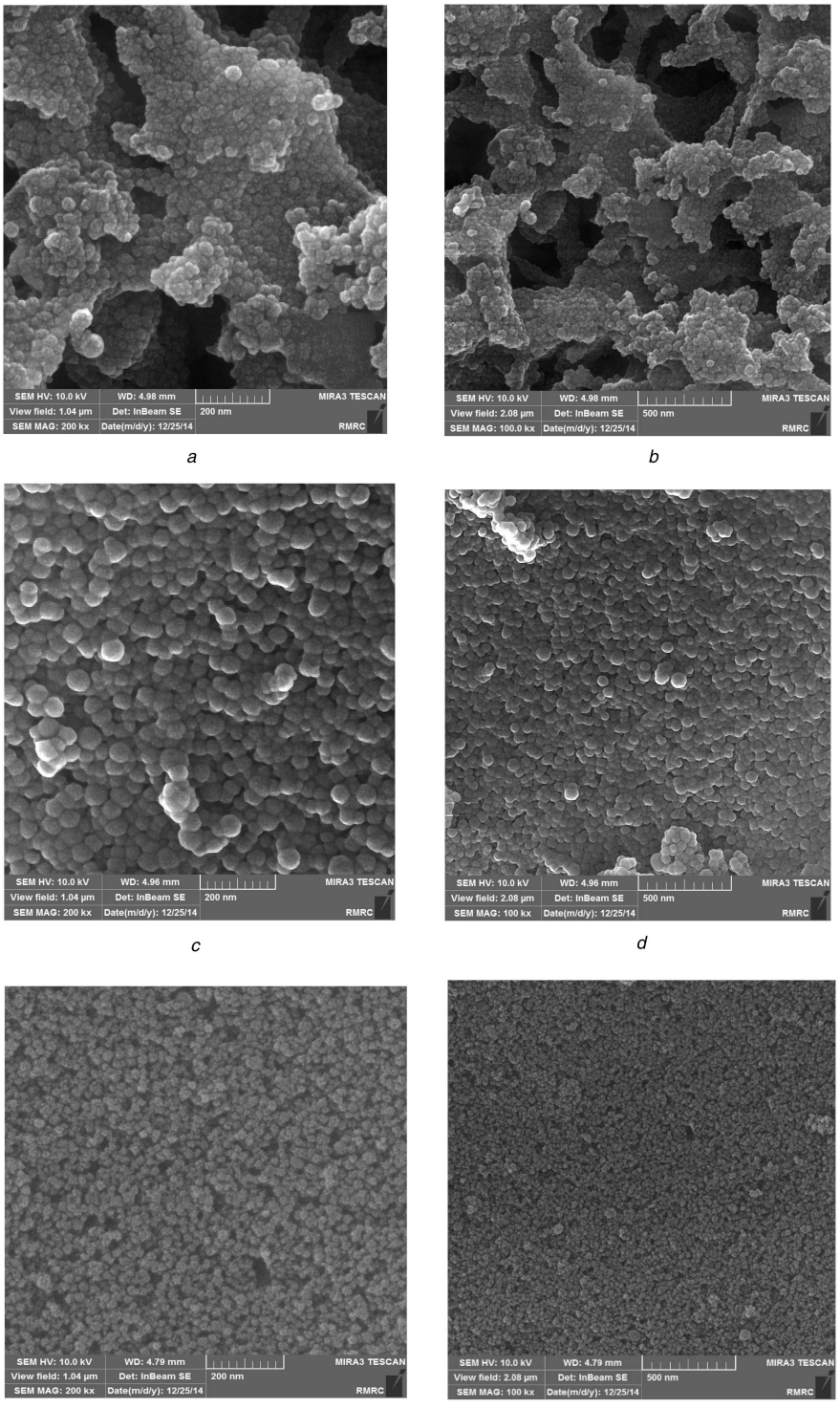

Fig. 2 *FE-SEM photograph of the MSNs*

(a, b) FE-SEM photography of unmodified MSNs(MCM-41-OH), ***(c, d)*** FE-SEM photography of modified MSNs with primary amines (MCM-41-NH_2), ***(e, f)*** FE-SEM photography of modified MSNs with imidazole groups (MCM-41-Im)

As shown in Fig. 4, the crystallinity of the synthesised samples was determined by XRD. The diffraction pattern exhibits clear peaks that can be indexed as (100) reflection 2.2 2θ. However, the broadened peaks related to 110 and 200 planes were scarcely identified, especially for MCM-41-Im.

The average particle size determined by DLS showed a similar result of 50 nm for MCM-41, 51 nm for MCM-41-NH_2, and 35 nm for MCM-41-Im. Table 3 shows an increased particle size of the modified MSNs after admixture with a pDNA solution that confirms complex formation. The electric potentials of MSNs at shear plane relative to the bulk dispersion medium away from the interface, or zeta-potential, were also determined. MCM-41 had a negative net charge of −3.8 mV. In contrast, the positive charges of +11.7 and +45.0 mV were observed for MCM-41-NH_2 and MCM-41-Im.

3.2 Interaction between plasmid DNA and MSN

In order to assess the complex formation, gel retardation assay was performed at varying *N*/*P* ratios of MSN to pDNA (0.1, 0.2, 0.5, 1, and 2). No pDNA migration happened in the gel for the *N*/*P* ratios as low as 0.2, similarly for MCM-41-NH_2 and MCM-41-Im (Fig. 5). In order to examine the ability of the modified MSNs to protect pDNA from enzymatic degradation, DNase-1 sample

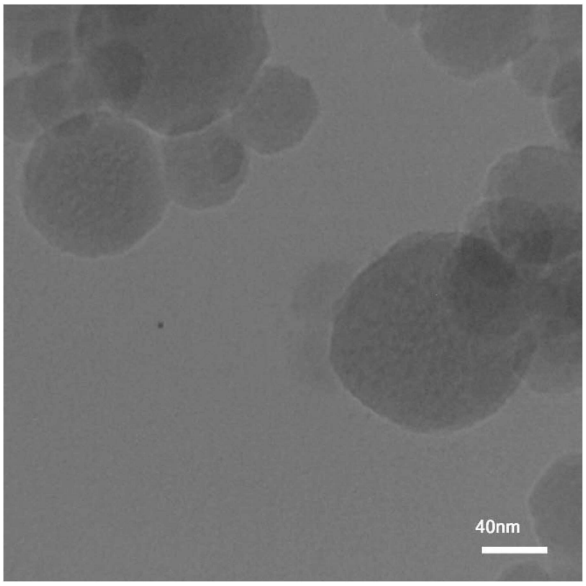

Fig. 3 *HRTEM photograph of modified MSN with imidazole (MCM-41-IM)*

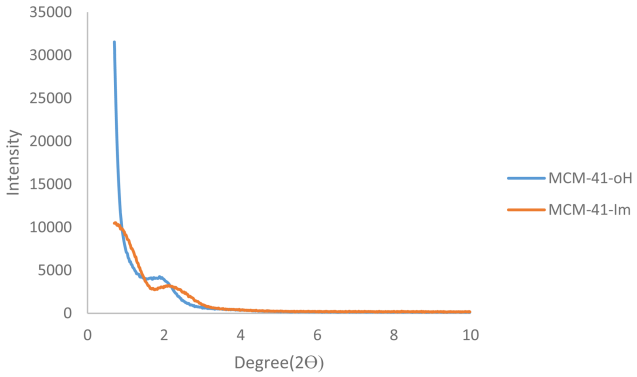

Fig. 4 *XRD pattern of the unmodified MCM-41 (MCM-41-OH) and the corresponding particles modified with imidazole (MCM-41-Im)*

Table 3 Mean hydrodynamic diameter and zeta potential of the synthesised mesoporous silica nanoparticles

Type of MSN	Hydrodynamic diameter, nm	Zeta potential, mV
MCM-41-OH	50.0	−3.8
MCM-41-NH_2	51.0	+11.7
MCM-41-IM	35.0	+45
MCM-41-NH_2/pDNA (*N*/*P* 1)	123.7	+4.5
MCM-41-Im/pDNA (*N*/*P* 1)	121.1	+7.1

treatments were carried out before gel electrophoresis for the complexes of pDNA with the modified MSNs at *N*/*P* ratios of 0.5 and 1 in comparison to free pDNA. Fig. 6 shows a complete degradation of free pDNA; however, the complexes of pDNA with the modified MSNs were retained in the wells. The level of pDNA protection was reliant on *N*/*P* ratio as well as the type of modification. As shown in Fig. 5, MCM-41-NH_2 had a weak interaction with pDNA as the intensity of pDNA band retained in the well was relatively lower than that of the MCM-41-Im complexes in the similar *N*/*P* ratio of 0.5.

3.3 Cellular experiments

In order to evaluate the safety of the synthesised MSNs before the cell transfection, MTT assay was performed in HeLa cells. The statistical results confirm dose-dependency of the cytotoxicity of different types of MSNs ($P < 0.001$), which was indicated by a decreasing percentage of live cells. Although there was no significant difference with respect to the type of MSN modification ($P = 0.896$) (Fig. 7*a*), the cytotoxic effect was only observed at concentrations higher than 3 µg/ml ($P < 0.01$).

MTT tests were also carried out to determine the viability of the cells treated with the pDNA/MSN complexes correspond to *N*/*P* ratios of 0.2, 0.5, 1, and 2. Fig. 7*b* shows an increase in cytotoxicity with increasing *N*/*P* ratio ($P < 0.05$). The cytotoxicity was significantly lower for the MCM-41-Im than the MCM-41-NH_2 complexes with pDNA ($P < 0.001$). Unlike naked E-GFP plasmid which did not show any significant cytotoxicity, the cell viability corresponding to Metafectene®/E-GFP plasmid was calculated 72% ± 4.6, though the difference from the modified MSNs was not determined significant ($P > 0.05$).

Gene transfer efficacy of MCM-41-NH_2 and MCM-41-Im loaded by pDNA was examined in vitro in HeLa cells. Fig. 8 shows the fluorescent cell percentage indicating expression of EGFP plasmid was significantly higher for the MCM-41-Im than MCM-41-NH_2 similarly at *N*/*P* ratios of 1 and 2 ($P < 0.001$), though there was no significant effect of *N*/*P* ratio of gene expression in the studied range ($P = 0.236$). Compared with Metafectene® as a positive control, MCM-41-Im showed a higher level of gene expression (~95%) at $N/P = 1$.

The flow cytometry method was used to investigate the particles' ability to escape from the endosomes following concomitant cell treatment with the modified MSNs and carboxyfluorescein as an endosomal tracer molecule. Unlike Fig. 9*a* which shows a similarly high carboxyfluorescein fluorescence induced by 1 mg/ml concentrations of MCM-41-NH_2 and MCM-41-Im (Fig. 9*b*), a superior fluorescence intensity was obtained at low concentration (0.5 mg/ml) of MCM-41-Im than MCM-41-NH_2 (Fig. 9*b*).

4 Discussion

High porosity structure, colloidal stability, and the possibility to functionalise the inner and/or the outer surface are among the features that make MCM-41 MSNs as good candidates for biological applications [43]. There are several previous studies that have shown that mesoporous silica nanoparticles could be endocytosed by mammalian cells [44, 45] and surfaces functionalised MSNs are suitable vehicle for intracellular control-released delivery [46, 47]. To investigate the application of the surface-modified MSNs in gene delivery as the main goal of the present study, a mandatory controlled synthesis needs to be undertaken to obtain spherical nanoparticles. Well-defined MCM-41 structures were synthesised according to reported procedure [43] with some modifications. To this end, MCM-41 bearing –NH_2 and imidazole functionalities (MCM-41-NH_2 and

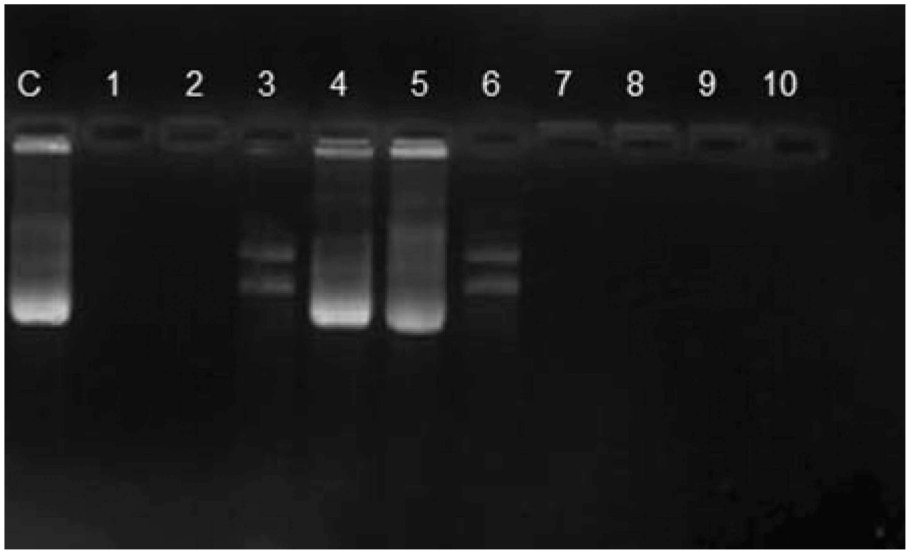

C. Free plasmid (Control)
1. MSN (NH2)/pDNA, N/P=1
2. MSN (NH2)/pDNA, N/P=0.5
3. MSN (NH2)/pDNA, N/P= 0.2
4. MSN (NH2)/pDNA, N/P= 0.1
5. MSN (IM)/pDNA, N/P =0.1
6. MSN (IM)/pDNA, N/P =0.2
7. MSN (IM)/pDNA, N/P =0.5
8. MSN (IM)/pDNA, N/P =1
9. MSN (IM)/pDNA, N/P =2
10. MSN (IM)/pDNA N/P =5

Fig. 5 *Agarose gel retardation assay of pDNA complexes with the modified MSNs in various N/P ratios (0.2, 0.5, 1, 2, and 5) in comparison to free pDNA*

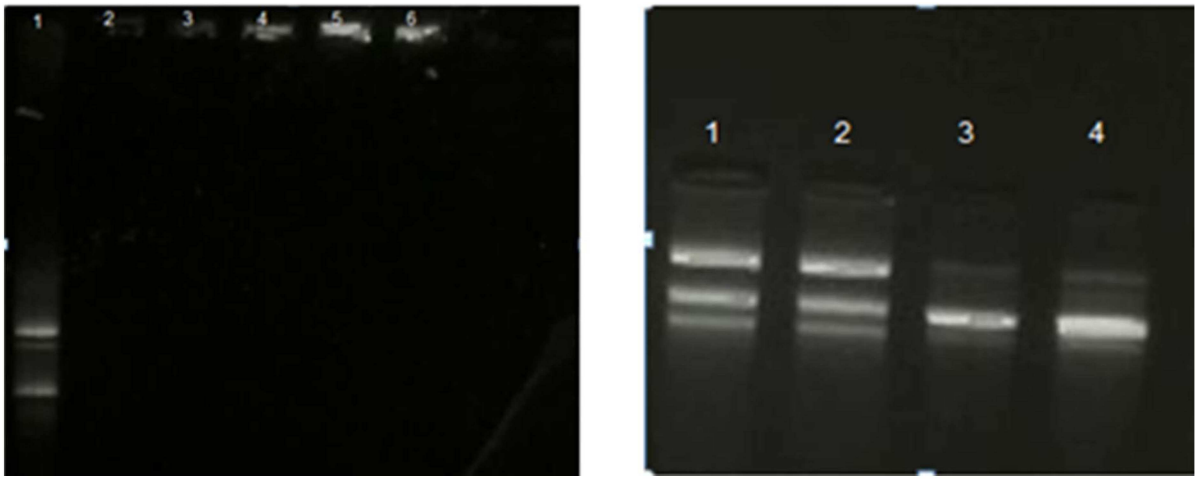

1. E-GFP plasmid (control)
2. Free plasmid
3. MCM-41NH_2/pDNA N/P=0.5
4. MCM-41NH_2 /pDNA N/P=1
5. MCM-41-Im/pDNA N/P=0.5
6. MCM-41-Im/pDNA N/P=1

a

1. MCM-41-Im/pDNA N/P=0.5
2. MCM-41-Im/pDNA N/P=1
3. MCM-41-NH2/pDNA N/P=0.5
4. MCM-41-NH2/pDNA N/P=1

b

Fig. 6 *DNase-I protection assay for modified MSNs with amine and imidazole groups*
(a) Agarose gel retardation assay after DNase-1 treatment of the samples: free pDNA or pDNA complexes with MCM-41-NH_2 or MCM-41-Im in *N/P* ratios of 0.5 and 1, ***(b)*** Retained pDNA in the wells that were extracted from the gel following DNase-1 treatment and investigated again by gel electrophoresis

MCM-41-Im) were synthesised by co-condensation method [48] and their applicability was investigated for pDNA condensation and transfection in HeLa cells.

The synthesised MSNs were characterised according to their size and morphology, crystallinity, porosity, chemical modifications, hydrodynamic diameter, and zeta-potentials. Aspherical particles of ~40 nm (Fig. 2) were obtained by the two-step method to control the rate of particle nucleation and growth [48]. XRD shows 100 planes, broadening of 110 and 200 planes attributed primarily to a decrease in the grain size [49] and also filling the pores of nanoparticles with the functional groups [50]. A little shift of 100 planes of MCM-41-Im XRD happened towards higher angles, demonstrating a decrease in the unit cell parameter (Fig. 4).

According to the BET, acquisition of the MSN samples possessing high SBET, Vt, and WBJH (Table 2) indicates their

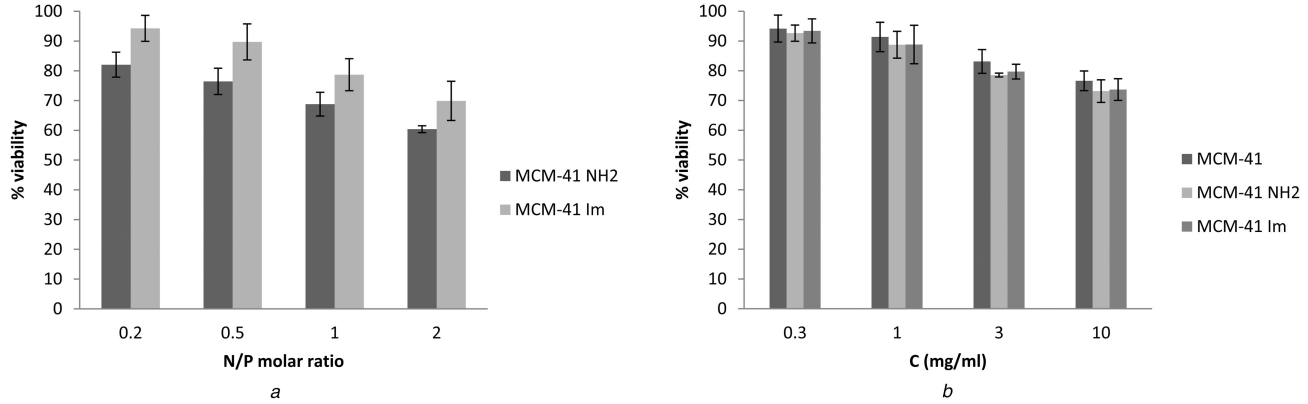

Fig. 7 *Cell viability of the modified MSNs as a function of MSN concentration*

(a) Cell viability of modified MSNs in complex with plasmid DNA in different N/P ratios of 0.2, 0.5, 1 and 2 in HeLa cells incubated after 48 h, ***(b)*** Cell viability of modified and unmodified MSNs with different concentrations of 0.3, 1, 3 and 10 mg/ml in HeLa cells incubated after 48 h

potential application for accumulating exogenous molecules as well as presenting surface functionalities. The MCM-41-OH showed the highest surface area of ∼1025 m^2/g while by introducing propylamine (MCM-41-NH_2) and propylimidazolium (MCM-41-Im) groups to inner pore walls, this value decreased to 975 m^2/g and 780, respectively, which are acceptable changes made by propylamine in compare with propylimidazolium groups.

The presence of –NH_2 and imidazole functional groups was confirmed by FTIR spectroscopy (Fig. 1) and CHN analysis (Table 1). As reported in the literature [51], DLS experiment showed a reduced particle size of silica nanoparticles following chemical modifications. Zeta potential of the modified MSNs demonstrated a decrease in the positive charges to the values of +4.5 and +7.2 mV for respective MCM-41-NH_2 and MCM-41-Im particles following incubation with pDNA (Table 3) that can be explained by electrostatic interactions happened between various amines and pDNA phosphates.

In some other studies, MSNs are synthesised with a pretty differences in method. Harini *et al*. synthesised MCM-41 in a one-step method and modified them after that. In this study, we tried to use co-condensation synthesis of MSNs in two-steps method and in terms of characterisation, we achieved smaller size of nanoparticles with sufficient functionality [52]. In another study, Kim *et al*. used MSNs for delivering BMP-2 plasmid DNA for in vitro osteogenic stimulation of mesenchymal stem cells. They synthesised MSN-NH_2 by modifying MCM-41 with APES with another different method and characteristics of products [35].

Interaction of the modified MSNs with pDNA results in retarding pDNA migration in gel electrophoresis [38]. This happens since the modified MSNs, unlike MCM-41-OH, bearing positive zeta potentials (Table 3) interacting with pDNA through electrostatic interactions to neutralise the negative charge of pDNA. Therefore, the pDNA complexes cannot migrate inside the electrical field of gel electrophoresis and are retained in the wells. The intensity of the band retained in the wells increased by the *N*/*P* mole ratio of pDNA/MSN (Fig. 5), confirming that pDNA retention is likely due to MSN interaction. However, the pDNA loaded on the modified MSNs in *N*/*P* mole ratio of >0.5 were retarded completely in the wells (Fig. 5), indicating strong complexes formed between pDNA and the functionalised MSNs at low *N*/*P* ratio. To verify the role of MSN modification, the experiment was also performed for unmodified MCM-41. Unlike the modified MCM-41, the bands corresponding to various forms of pDNA were observed in the gel, showing that MCM-41 without further surface modification cannot interact with pDNA successfully. The incomplete interactions of pDNA and the MSNs at *N*/*P* ratios <0.5 were also noticed by a partial migration of pDNA in the gel. In comparison to the similar report on the application of histidine functionalised MSNs for plasmid delivery [34], more tightly condensed complexes are formed between pDNA and MCM-41-Im. Also, a relatively lower amount of MCM-41-Im is required to attain a complete complex formation in comparison to histidine modified MSN [53]. Dissimilar synthesis method or the different relative amount of imidazole functional groups used in the preparation of the modified MSNs may explain variable presentation of imidazole groups interacting to pDNA on the MCM-41 surface.

Moreover, MCM-41-Im complexes with pDNA resist against DNase1 degradation (Fig. 6), which may be due to the role of the imidazole groups in condensation of pDNA. Considering that apparent pKa of imidazole is ∼6.5 and it is partially protonated in deionised water [54], the formation of some hydrophobic regions on MCM-41-Im surface due to the presence of a unprotonated form of imidazole amine group may contribute to a better condensation of pDNA and a more resistance to DNase 1 digestion. The mutual contribution of electrostatic and hydrophobic interactions in DNA condensation has been discussed elsewhere [55].

The cytotoxicity of free MSNs and MS *N*/*P* DNA complexes were investigated by MTT assay. Similar cytotoxic profiles were obtained for all free MSNs in HeLa cells (Fig. 7). Lin *et al.* [56] have also demonstrated a comparable dose-dependent cytotoxicity of 15 nm silica nanoparticles at a concentration >10 µg/ml in lung adenocarcinoma cells. In another study, the size-dependent cytotoxicity of MSN particles has been addressed [57] that the smaller particles show a lower cytotoxicity. However, the size of reported particles has been above the size range used in the present study. Unlike free MSNs, less cytotoxic complexes were found between pDNA and MCM-41-Im than MCM-41-NH_2 possibly due to a more membrane-disrupting activity of protonated primary amines [42]. This finding is not consistent with a recent report on the application of MSN-NH_2 and histidine-conjugated MSNs for gene delivery application [34] that no significant difference has been noticed between these modifications and at various *N*/*P* mole ratios, showing the plausible participation of available NH_2 group of L-histidine in the cytotoxicity of the conjugated MSNs.

Transfection efficiency of the modified MSNs was investigated by flow cytometry (Fig. 8). The results show a superior cell-associated EGFP fluorescence following incubation with MCM-41-Im/pDNA complexes than the complexes of pDNA with MCM-41-NH_2 or Metafectene® (a standard transfecting agent) that might be attributed to enhance cellular uptake and/or endosomal escape caused by imidazole groups [58, 59]. Surface functionalisation of the MSNs with either –NH_2 or imidazole group results in increasing pDNA condensation (Fig. 5) and formation of the loaded particles with a mean hydrodynamic diameter of ∼120 nm and few positive charges (Table 3) that is assumed to induce cellular uptake and expression of EGFP plasmid [60]. Since making a balance between cationic density of nanoparticles and their charge density causes better cellular interaction and endocytosis [60, 61], in the present study, *N*/*P* ratio as the molar ratio of amine group of modified MSNs to DNA phosphate groups was used for making this balance. To demonstrate the capability of the modified MSNs to escape from the endosome as a prerequisite step for pDNA transfection, flow cytometry was performed.

Carboxyfluorescein was used as a negatively charged, membrane impermeable fluorescent tracer that is internalised by

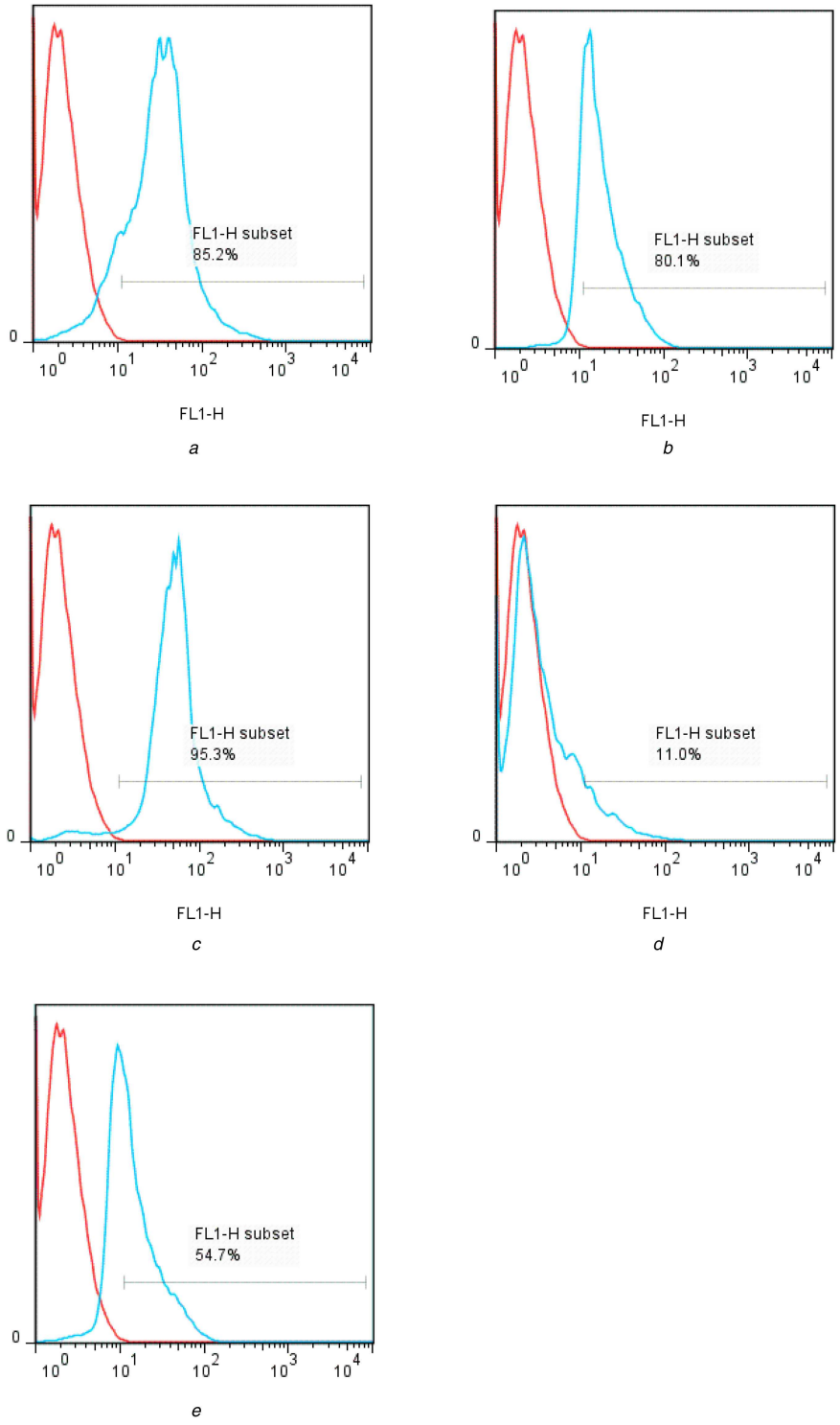

Fig. 8 *Flow cytometry analysis of E-GFP plasmid gene expression in HeLa cell transfected with*
(a) Metafectene®, ***(b)*** MCM-41-Im, $N/P = 0.5$, ***(c)*** MCM-41-Im, $N/P = 1$, ***(d)*** MCM-41-NH_2, $N/P = 0.5$, ***(e)*** MCM-41-NH_2, $N/P = 1$ (blue lines) versus negative control cells (red lines)

the cells only via endocytosis. The fluorescence of carboxyfluoresce is self-quenched at the intra-endosomal high concentrations used in the present study, but their escape from the endosomes can be monitored by fluorescence dequenching. Similar to another report [60], imidazole groups cause a better endosomal escape than $-NH_2$, which is only noticeable at the low MSN concentration (Fig. 9*a*). This result is consistent with the higher gene expression obtained for MCM-41-Im that confirms the involvement of imidazole groups in the enhanced endosomal escape, cyto-compatibility of pDNA complexes (Fig. 7*b*) and the higher transfection efficiency of MCM-41-Im in an optimum *N*/*P* ratio (Fig. 8).

5 Conclusion

Through this study, the sized controlled MSNs particles are recognised as novel carriers for gene transfection. The co-condensation method applied to develop the modified MCM-41 nanoparticles showed a clear improvement in pDNA condensation, protection against DNase-1 digestion, and improved transfection efficiency. Both functionalised MSNs, MCM-41-HN2 and MCM-41-im, showed excellent performance in pDNA transfection which observed in flow cytometry results. However, better transfection was observed by MCM-41-Im due to the presence of more effective functional groups of imidazolium with more positive charge. Furthermore, other functionalisation of MSNs

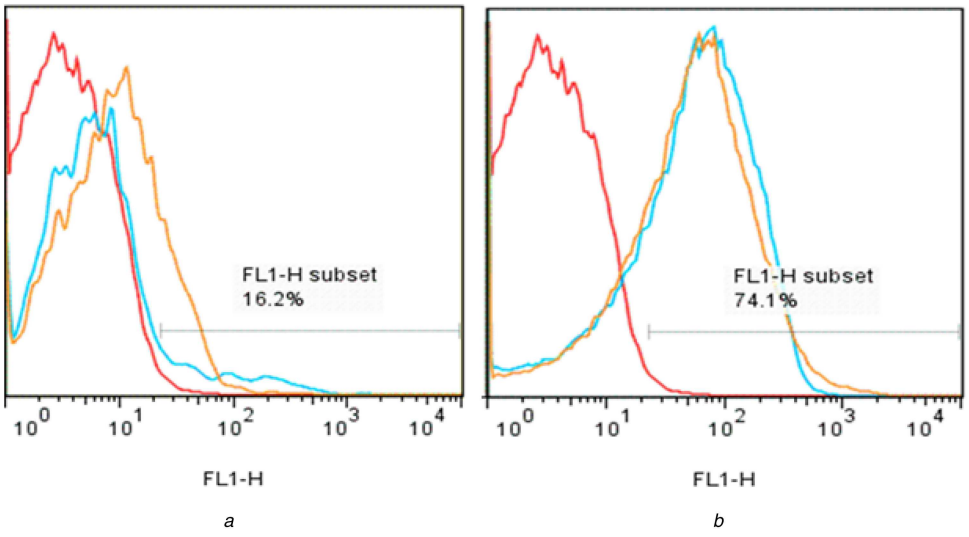

Fig. 9 *Flow cytometry analysis of endosomal escape using dequenching of carboxyfluorescein alone (negative control, red lines) in HeLa cells or following co-incubation with*
(a) 0.5 mg/ml or ***(b)*** 1 mg/ml MCM-41-Im (blue lines) and MCM-41-NH_2 (orange lines)

could be done using silane coupling agents for receptor-mediated gene transfer with specific ligands that could be recognised by target cell biomarkers. Furthermore, safety and efficacy of the modified MSNs have to be tested in vivo to investigate their success as a gene carrier in overcoming extracellular and intracellular barriers.

6 Acknowledgments

The authors thank the staff of Center for Nanotechnology in Drug Delivery, School of Pharmacy and Paramedical School, Reza Ranjbaran and Mohammad-Ali Okhovat, for their contribution to the project. This work is a part of Ms. Mahmoodi thesis (grant # 6633) financially supported by a research grant from Shiraz University of Medical Sciences.

7 References

[1] Mulligan, R.C.: 'The basic science of gene therapy', *Science*, 1993, **260**, (5110), pp. 926–932
[2] Verma, I.M., Somia, N.: 'Gene therapy-promises, problems and prospects', *Nature*, 1997, **389**, (6648), pp. 239–242
[3] Vijayanathan, V., Thomas, T., Thomas, T.: 'DNA nanoparticles and development of DNA delivery vehicles for gene therapy', *Biochemistry*, 2002, **41**, (48), pp. 14085–14094
[4] Wang, W., Li, W., Ma, N., *et al.*: 'Non-viral gene delivery methods', *Current Pharm. Biotechnol.*, 2013, **14**, (1), pp. 46–60
[5] Niidome, T., Huang, L.: 'Gene therapy progress and prospects: nonviral vectors', *Gene therapy*, 2002, **9**, (24), p. 1647
[6] Dobson, J.: 'Magnetic micro-and nano-particle-based targeting for drug and gene delivery', *Nanomedicine*, 2006, **1**, (1), pp. 31–37
[7] Liu, C., Zhang, P., Zhai, X., *et al.*: 'Nano-carrier for gene delivery and bioimaging based on carbon dots with PEI-passivation enhanced fluorescence', *Biomaterials*, 2012, **33**, (13), pp. 3604–3613
[8] Kafshdooz, T., Kafshdooz, L., Akbarzadeh, A., *et al.*: 'Applications of nanoparticle systems in gene delivery and gene therapy', *Artif. Cells Nanomed. Biotechnol.*, 2016, **44**, (2), pp. 581–587
[9] Pandey, A.P., Singh, S.S., Patil, G.B., *et al.*: 'Sonication-assisted drug encapsulation in layer-by-layer self-assembled gelatin-poly (styrenesulfonate) polyelectrolyte nanocapsules: process optimization', *Artif. Cells Nanomed. Biotechnol.*, 2015, **43**, (6), pp. 413–424
[10] Couvreur, P., Vauthier, C.: 'Nanotechnology: intelligent design to treat complex disease', *Pharm. Res.*, 2006, **23**, (7), pp. 1417–1450
[11] Ganta, S., Devalapally, H., Shahiwala, A., *et al.*: 'A review of stimuli-responsive nanocarriers for drug and gene delivery', *J. Control. Release*, 2008, **126**, (3), pp. 187–204
[12] Gao, X., Cui, Y., Levenson, R.M., *et al.*: 'In vivo cancer targeting and imaging with semiconductor quantum dots', *Nat. Biotechnol.*, 2004, **22**, (8), pp. 969–976
[13] Khan, J.A., Pillai, B., Das, T.K., *et al.*: 'Molecular effects of uptake of gold nanoparticles in HeLa cells', *ChemBioChem*, 2007, **8**, (11), pp. 1237–1240
[14] Moghimi, S.M., Hunter, A.C., Murray, J.C.: 'Nanomedicine: current status and future prospects', *FASEB J.*, 2005, **19**, (3), pp. 311–330
[15] Tamaddon, A.M., Shirazi, F.H., Moghimi, H.R.: 'Modeling cytoplasmic release of encapsulated oligonucleotides from cationic liposomes', *Int. J. Pharm.*, 2007, **336**, (1), pp. 174–182
[16] Emerich, D.F., Thanos, C.G.: 'Nanotechnology and medicine', *Expert Opin. Biol. Ther.*, 2003, **3**, (4), pp. 655–663
[17] Golkar, N., Samani, S.M., Tamaddon, A.M.: 'Cholesterol-conjugated supramolecular assemblies of low generations polyamidoamine dendrimers for enhanced EGFP plasmid DNA transfection', *J. Nanoparticle Res.*, 2016, **18**, (5), pp. 1–20
[18] De, M., Ghosh, P.S., Rotello, V.M.: 'Applications of nanoparticles in biology', *Adv. Mater.*, 2008, **20**, (22), pp. 4225–4241
[19] Rejeeth, C., Vivek, R.: 'Comparison of two silica based nonviral gene therapy vectors for breast carcinoma: evaluation of the p53 delivery system in balb/c mice', *Artif. Cells Nanomed. Biotechnol.*, 2017, **45**, (3), pp. 1–6
[20] Slowing, I.I., Trewyn, B.G., Giri, S., *et al.*: 'Mesoporous silica nanoparticles for drug delivery and biosensing applications', *Adv. Funct. Mater.*, 2007, **17**, (8), pp. 1225–1236
[21] Slowing, I.I., Vivero-Escoto, J.L., Wu, C.-W., *et al.*: 'Mesoporous silica nanoparticles as controlled release drug delivery and gene transfection carriers', *Adv. Drug Deliv. Rev.*, 2008, **60**, (11), pp. 1278–1288
[22] Alidadiyani, N., Salehi, R., Ghaderi, S., *et al.*: 'Synergistic antiproliferative effects of methotrexate-loaded smart silica nanocomposites in MDA-MB-231 breast cancer cells', *Artif. Cells Nanomed. Biotechnol.*, 2016, **44**, (2), pp. 603–609
[23] Barkalina, N., Jones, C., Kashir, J., *et al.*: 'Effects of mesoporous silica nanoparticles upon the function of mammalian sperm in vitro', *Nanomed. Nanotechnol. Biol. Med.*, 2014, **10**, (4), pp. 859–870
[24] Hudson, S.P., Padera, R.F., Langer, R., *et al.*: 'The biocompatibility of mesoporous silicates', *Biomaterials*, 2008, **29**, (30), pp. 4045–4055
[25] Lu, J., Liong, M., Li, Z., *et al.*: 'Biocompatibility, biodistribution, and drug-delivery efficiency of mesoporous silica nanoparticles for cancer therapy in animals', *Small*, 2010, **6**, (16), pp. 1794–1805
[26] Hanafi-Bojd, M.Y., Jaafari, M.R., Ramezanian, N., *et al.*: 'Surface functionalized mesoporous silica nanoparticles as an effective carrier for epirubicin delivery to cancer cells', *Eur. J. Pharm. Biopharm.*, 2015, **89**, pp. 248–258
[27] Kar, M., Tiwari, N., Tiwari, M., *et al.*: 'Poly-L-arginine grafted silica mesoporous nanoparticles for enhanced cellular uptake and their application in DNA delivery and controlled drug release', *Part. Part. Syst. Charact.*, 2013, **30**, (2), pp. 166–179
[28] Park, I.Y., Kim, I.Y., Yoo, M.K., *et al.*: 'Mannosylated polyethylenimine coupled mesoporous silica nanoparticles for receptor-mediated gene delivery', *Int. J. Pharm.*, 2008, **359**, (1), pp. 280–287
[29] Tumturk, H., Yüksekdag, H.: 'Acetylcholinesterase immobilized onto PEI-coated silica nanoparticles', *Artif. Cells Nanomed. Biotechnol.*, 2016, **44**, (2), pp. 443–447
[30] Xia, T., Kovochich, M., Liong, M., *et al.*: 'Polyethyleneimine coating enhances the cellular uptake of mesoporous silica nanoparticles and allows safe delivery of siRNA and DNA constructs', *ACS Nano*, 2009, **3**, (10), pp. 3273–3286
[31] Shen, J., Kim, H.-C., Su, H., *et al.*: 'Cyclodextrin and polyethylenimine functionalized mesoporous silica nanoparticles for delivery of siRNA cancer therapeutics', *Theranostics*, 2014, **4**, (5), pp. 487–497
[32] Bhattarai, S.R., Muthuswamy, E., Wani, A., *et al.*: 'Enhanced gene and siRNA delivery by polycation-modified mesoporous silica nanoparticles loaded with chloroquine', *Pharm. Res.*, 2010, **27**, (12), pp. 2556–2568
[33] Hartono, S.B., Gu, W., Kleitz, F., *et al.*: 'Poly-L-lysine functionalized large pore cubic mesostructured silica nanoparticles as biocompatible carriers for gene delivery', *ACS Nano*, 2012, **6**, (3), pp. 2104–2117
[34] Brevet, D., Hocine, O., Delalande, A., *et al.*: 'Improved gene transfer with histidine-functionalized mesoporous silica nanoparticles', *Int. J. Pharm.*, 2014, **471**, (1), pp. 197–205
[35] Kim, T.H., Kim, M., Eltohamy, M., *et al.*: 'Efficacy of mesoporous silica nanoparticles in delivering BMP-2 plasmid DNA for in vitro osteogenic

stimulation of mesenchymal stem cells', *J. Biomed. Mater. Res. Part A*, 2013, **101**, (6), pp. 1651–1660
[36] Farjadian, F., Ahmadpour, P., Samani, S.M., *et al.*: 'Controlled size synthesis and application of nanosphere MCM-41 as potent adsorber of drugs: a novel approach to new antidote agent for intoxication', *Microporous Mesoporous Mater.*, 2015, **213**, pp. 30–39
[37] Farjadian, F., Ghasemi, S., Heidari, R., *et al.*: 'In vitro and in vivo assessment of EDTA-modified silica nano-spheres with supreme capacity of iron capture as a novel antidote agent', *Nanomed. Nanotechnol. Biol. Med.*, 2017, **13**, (2), pp. 745–753
[38] Najafi, H., Abolmaali, S.S., Owrangi, B., *et al.*: 'Serum resistant and enhanced transfection of plasmid DNA by PEG-stabilized polyplex nanoparticles of L-histidine substituted polyethyleneimine', *Macromol. Res.*, 2015, **23**, (7), pp. 618–627
[39] Golkar, N., Samani, S.M., Tamaddon, A.M.: 'Data on cell growth inhibition induced by anti-VEGF siRNA delivered by stealth liposomes incorporating G2 PAMAM-cholesterol versus Metafectene® as a function of exposure time and siRNA concentration', *Data Brief*, 2016, **8**, pp. 1018–1023
[40] Abolmaali, S.S., Tamaddon, A.M., Mohammadi, S., *et al.*: 'Chemically crosslinked nanogels of PEGylated poly ethyleneimine (l-histidine substituted) synthesized via metal ion coordinated self-assembly for delivery of methotrexate: cytocompatibility, cellular delivery and antitumor activity in resistant cells', *Mater. Sci. Eng. C*, 2016, **62**, pp. 897–907
[41] Beganskienė, A, Sirutkaitis, V, Kurtinaitienė, M, *et al.*: 'FTIR, TEM and NMR investigations of Stöber silica nanoparticles', *Mater. Sci. (Medžiagotyra)*, 2004, **10**, pp. 287–290
[42] Abolmaali, S.S., Tamaddon, A., Najafi, H., *et al.*: 'Effect of l-histidine substitution on sol–gel of transition metal coordinated poly ethyleneimine: synthesis and biochemical characterization', *J. Inorg. Organomet. Polym. Mater.*, 2014, **24**, (6), pp. 977–987
[43] Lin, Y.-S., Tsai, C.-P., Huang, H.-Y., *et al.*: 'Well-ordered mesoporous silica nanoparticles as cell markers', *Chem. Mater.*, 2005, **17**, (18), pp. 4570–4573
[44] Huang, D.-M., Hung, Y., Ko, B.-S., *et al.*: 'Highly efficient cellular labeling of mesoporous nanoparticles in human mesenchymal stem cells: implication for stem cell tracking', *FASEB J.*, 2005, **19**, (14), pp. 2014–2016
[45] Slowing, I., Trewyn, B.G., Lin, V.S.-Y.: 'Effect of surface functionalization of MCM-41-type mesoporous silica nanoparticles on the endocytosis by human cancer cells', *J. Am. Chem. Soc.*, 2006, **128**, (46), pp. 14792–14793
[46] Gruenhagen, J.A., Lai, C.-Y., Radu, D.R., *et al.*: 'Real-time imaging of tunable adenosine 5-triphosphate release from an MCM-41-type mesoporous silica nanosphere-based delivery system', *Appl. Spectrosc.*, 2005, **59**, (4), pp. 424–431
[47] Lai, C.-Y., Trewyn, B.G., Jeftinija, D.M., *et al.*: 'A mesoporous silica nanosphere-based carrier system with chemically removable CdS nanoparticle caps for stimuli-responsive controlled release of neurotransmitters and drug molecules', *J. Am. Chem. Soc.*, 2003, **125**, (15), pp. 4451–4459
[48] Huh, S., Wiench, J.W., Yoo, J.-C., *et al.*: 'Organic functionalization and morphology control of mesoporous silicas via a co-condensation synthesis method', *Chem. Mater.*, 2003, **15**, (22), pp. 4247–4256
[49] Ikari, K., Suzuki, K., Imai, H.: 'Structural control of mesoporous silica nanoparticles in a binary surfactant system', *Langmuir*, 2006, **22**, (2), pp. 802–806
[50] Bolouki, A., Rashidi, L., Vasheghani-Farahani, E., *et al.*: 'Study of mesoporous silica nanoparticles as nanocarriers for sustained release of curcumin', *Int. J. Nanosci. Nanotechnol.*, 2015, **11**, (3), pp. 139–146
[51] Demadis, K.D., Brückner, S.I., Brunner, E., *et al.*: 'The intimate role of imidazole in the stabilization of silicic acid by a pH-responsive, histidine-grafted polyampholyte', *Chem. Mater.*, 2015, **27**, (19), pp. 6827–6836
[52] Harini, L., Karthikeyan, B., Srivastava, S., *et al.*: 'Polyethylenimine-modified curcumin-loaded mesoporus silica nanoparticle (MCM-41) induces cell death in MCF-7 cell line', *IET Nanobiotechnol.*, 2016, **11**, (1), pp. 57–61
[53] Choi, E.W., Shin, I.S., Chae, Y.J., *et al.*: 'Effects of GM-CSF gene transfer using silica-nanoparticles as a vehicle on white blood cell production in dogs', *Exp. Hematol.*, 2008, **36**, (7), pp. 807–815
[54] Wang, C.Y., Huang, L.: 'Polyhistidine mediates an acid-dependent fusion of negatively charged liposomes', *Biochemistry*, 1984, **23**, (19), pp. 4409–4416
[55] Matulis, D., Rouzina, I., Bloomfield, V.A.: 'Thermodynamics of cationic lipid binding to DNA and DNA condensation: roles of electrostatics and hydrophobicity', *J. Am. Chem. Soc.*, 2002, **124**, (25), pp. 7331–7342
[56] Lin, W., Huang, Y.-w., Zhou, X.-D., *et al.*: 'In vitro toxicity of silica nanoparticles in human lung cancer cells', *Toxicol. Appl. Pharmacol.*, 2006, **217**, (3), pp. 252–259
[57] Vallhov, H., Gabrielsson, S., Strømme, M., *et al.*: 'Mesoporous silica particles induce size dependent effects on human dendritic cells', *Nano Lett.*, 2007, **7**, (12), pp. 3576–3582
[58] Midoux, P., Pichon, C., Yaouanc, J.J., *et al.*: 'Chemical vectors for gene delivery: a current review on polymers, peptides and lipids containing histidine or imidazole as nucleic acids carriers', *Br. J. Pharmacol.*, 2009, **157**, (2), pp. 166–178
[59] Varkouhi, A.K., Scholte, M., Storm, G., *et al.*: 'Endosomal escape pathways for delivery of biologicals', *J. Control. Release*, 2011, **151**, (3), pp. 220–228
[60] Putnam, D., Gentry, C.A., Pack, D.W., *et al.*: 'Polymer-based gene delivery with low cytotoxicity by a unique balance of side-chain termini', *Proc. Natl Acad. Sci. USA*, 2001, **98**, (3), pp. 1200–1205
[61] Clark, R.A., Olsson, I., Klebanoff, S.J.: 'Cytotoxicity for tumor cells of cationic proteins from human neutrophil granules', *J. Cell Biol.*, 1976, **70**, (3), pp. 719–723